Organics adsorption on novel amorphous silica and silica xerogels: Micro Column Rapid Breakthrough test coupled with Sequential Injection Analysis

Andrea Luca Tasca[a]*, Ashleigh J. Fletcher[a], Fernando Maya Alejandro[c], Farnaz Ghajeri[b], Gemma Turnes Palomino[c]

[a] Department of Chemical and Process Engineering, University of Strathclyde, Glasgow G1 1XJ, United Kingdom

[b] Department of Engineering Sciences, Applied Materials Science, Uppsala University, Uppsala, Sweden

[c] Department of Chemistry, Faculty of Sciences, University of the Balearic Islands, Carretera de Valldemossa km 7.5, E-07122 Palma de Mallorca, Illes Balears, Spain

* andrea.tasca@strath.ac.uk

Abstract

The adsorption capacities of a novel amorphous silica, and silica xerogels, for aromatic compounds were investigated using Micro Column Rapid Breakthrough tests coupled with Sequential Injection Flow-based automated instrumentation, in order to evaluate their operative feasibility under conditions typically used in water treatment facilities. Extraction columns were fabricated using stereolithographic 3D printing. Sorbent reusability was also investigated using automated flow-based techniques. Benzene was selected as target dissolved organic compound usually present in produced waters from the oil and gas sector, continuously increasing. 3,4-dichloroaniline (3,4-DCA) was selected as part of Endocrine Disrupting Chemicals, which are becoming source of major concern for human and wildlife toxicity. Novel amorphous silica were synthesised at low temperature and under ambient

pressure from a sodium metasilicate precursor, and were subject to post-synthetic methylation. Silica xerogels were prepared via acid catalysis of a sodium metasilicate solution and functionalised with trimethylchlorosilane, at low temperature and under ambient pressure. The removal efficiency of the silica xerogels tested was found equal greater than 22.62 mg/g for benzene at a flow rate of 0.6 mL/min, while the uptake of 3,4-DCA was found >4.63 mg/g and >7.17 mg/g, respectively at flow rates of 1.8 mL/min and 0.6 mL/min.

Keywords

SIA; SPE; 3,4-DCA; EDCs; 3D printing; benzene; breakthrough curves

1 Introduction

Global demand on clean water supplies is becoming increasingly intensive, thus the need for innovative and cost effective water treatment technologies is rising, including those designed to treat produced water from oil exploration activities. Produced water is the largest by-product generated by oil and gas extraction; hence, there are significant quantities of contaminated water that require remediation. Additional stress has been placed on this valuable resource by the presence of further organics known as Endocrine Disrupting Chemicals (EDCs), which have been detected at increasing levels in various sewage discharges, fresh- and estuarine-waters in recent years, and are, therefore of increasing concern for water agencies (Bevan et al., 2012, Kortenkamp et al., 2007).

Membranes are a promising but expensive technology for water remediation, however, the use of an adsorption media as a prior treatment could make them a potentially cost-effective option. Within the range of available solid sorbents, hydrophobic aerogels and xerogels

exhibit very attractive properties for oil spill remediation (Reynolds et al., 2001a, Reynolds et al., 2001b, Adebajo et al., 2003, Wang et al., 2012, Olalekan et al., 2014). However, very few studies have investigated the adsorption performance of hydrophobic gels at the low organic concentrations typical of water treatment applications (Simpson et al., 1993, Wang et al., 2011, Tasca et al., 2017), while the costs associated with functionalisation of these materials currently hinder their use as sorbents in the final stages of produced water treatments. It is also notable that the majority of previous work on organics adsorption from aqueous phase has been limited to batch tests, which fails to assess the feasibility of the materials developed as sorbents in apparatus commonly used in water treatment plants.

Column breakthrough experiments are crucial in identifying sorbent capacity, allowing estimation of material utilisation rate and treatment costs. The first recorded breakthrough experiments employed non-sieved sorbents and high flow rates in order to guarantee the same empty bed contact time (EBCT, defined as the ratio between the bed volume and the flowrate applied) employed in treatment facilities, where long exposure times and large sample volumes are required. Such experimental regimes have not always been practicable, hence, advanced studies were subsequently performed using small (>100 g), mini (>5 g) and then micro (<2 g) columns (Chang et al., 2007), while Rapid Small Scale Column Tests (RSSCT) were specifically developed to provide an estimate of the operative capacities of granular activated carbons (ASTM, 2008). The underlying theory behind RSSCT and all Micro-Column Breakthrough (MCRB) techniques is the appropriate scaling of hydrodynamic and mass transfer characteristics to small scale flow test column dimensions, assuming that the breakthrough curves would be similar to those of a pilot scale plant. Such tests mean that only minimal quantities of water and time are required to simulate pilot scale studies (Ying et al., 2006).

Recent improvements to MCRB methods were recently introduced by the use of low cost sampler, piping, fittings, and pumps, to obtain data on the adsorption of phenol, methyl tert-butyl ether, and other organic pollutants on carbon (Chang et al., 2007). In tandem with these improvements, sequential-injection analysis (SIA) has been shown to overcome the some limitations of classic flow-injection analysis (FIA), mainly related to complex manifold operations (Shu and Chung, 2017, Falkova et al., 2016). As such, SIA simplifies the sample manipulation required before measurement steps, and includes in-line sample dilution, dialysis and gas diffusion, enzymatic and immunological testing, as well as extraction (Economou, 2005). Additional gains in ease of analysis can be made by avoiding traditional solid-phase extraction, which is time-consuming, reagent intensive and produces significant waster, instead using automated solid phase extraction, which is quicker, requires little manipulation by the analyst, reduces reagent consumption and, consequently, minimises waste generation (Rodríguez et al., 2016).

This work uses advanced adsorption methods to study the uptake of benzene, as representative of dissolved oil species in produced water, on hydrophilic and hydrophobic amorphous silica and silica xerogels synthesised under ambient pressure and at low temperature conditions. Results are also presented for adsorption of 3,4-dichloroaniline on the aforementioned materials, using both batch and MCRB tests coupled with SIA. Additional automated solid-phase extraction was used for desorbing the organics from the materials. The column used for the MCRB test was 3D printed on methacrylate. Three-dimensional (3D) printing is a layer upon layer fabrication technology which uses material deposition in order to build up different geometrical shape of 3D components (Hwa et al., 2017), most commonly from a stereolithography (STL) file (Mitsouras et al., 2015) and with no intermediate steps, thus minimising labour, time and costs (Hampson et al., 2018).

2 Materials and methods

2.1 3D printing of the column

To design the column was used the 3D modelling tool for designers Rhinoceros 5, developed by Robert McNeel & Associates. The inside components of the column were created one by one and combined using Boolean operators. The model of the column was then extracted as a STL file and loaded in the software preForm, provided by FormLabs. A Form1+ 3D printer from FormLabs (tech specs) was used to printing the model on clear methacrylate photopolymer, while a CL-1000 ultraviolet crosslinker was adopted to finish the cure process.

2.2 Adsorbent synthesis

2.2.1 Quartzene

Quartzene is a novel amorphous silica; samples used in this study were supplied by Svenska Aerogel AB (SvAAB) and offered a range of silicas with hydrophilic nature (ND, Z1 and CMS), and their hydrophobic analogues (NDH, Z1H and CMSH). Hydrophilicity and hydrophobicity of Quartzene can be tailored to suit the desired application, and its porous structure can also be controlled, notably without the addition of any surfactant. Unlike traditional aerogels, the material is cheap to produce and is prepared via an environmentally friendly synthetic procedure, by virtue of the temperature and pressure conditions used. The synthetic procedure for Quartzene has been reported previously (Bangi et al., 2009); in summary, ND type Quartzene was prepared via the precipitation of sodium metasilicate (SiO_2:Na_2O = 3.35) with sodium chloride, where after, the precipitate was mixed with tap water, before vacuum filtration, and the resulting paste, comprising up to 85% water, was spray-dried. Z1 samples were prepared using a method analogous to that for ND, but with a different level of activation of the silica source (Twumasi Afriyie et al., 2014). CMS samples were prepared by mixing magnesium chloride hexahydrate (68 mol% Mg) and calcium

chloride dihydride (32 mol% Ca) before adding to a sodium metasilicate solution, at a concentration ratio of 1:2. Coagulation occurred, as previously described (Twumasi Afriyie et al., 2013), and the resulting gel was washed, filtered and dried, as described for ND samples. Hydrophobic NDH, Z1H and CMSH were prepared, by SvAAB, via methylation of the hydrophilic analogues.

2.2.2 Silica xerogels

Silica xerogels were synthesised using diluted solutions of sodium metasilicate, as inspired by the work of Bangi *et al.* (Bangi et al., 2009); the commercial solution has formulation $(NaOH)_x(Na_2SiO_3)_y*zH_2O$, ≥10%NaOH basis and ≥27%SiO_2 basis, and was diluted with distilled water to produce H_2O:Na_2SiO_3 molar ratios from 80 to 200. Acid catalysis was performed by dropwise addition of citric acid (3 M), to 40 mL of 10%vol diluted sodium silicate solution placed in a 400 mL cylindrical glass container and manually stirred during the addition. Containers were subsequently placed in oven at 323 K, partially covered, for gelation and a first drying phase to occur. Consecutive washing, solvent exchange, and hydrophobisation were chosen to minimize consumption of the hydrophobisation agent. 24 h post acid addition, the dried gels were washed 3 times in 24 h, after first being cut into small pieces (~1 cm cubes) in order to speed up the exchange of sodium ions with distilled water. Water was then exchanged with methanol, prior to functionalisation with a mixture of 1:1:1 volume of hexane, TMCS and methanol. Samples were placed in the oven at 323 K during washing, methanol exchange and functionalisation. Finally, curing for 1 d at room temperature and 1 h in an oven at 473 K completed the synthesis. Similar gels were synthesised without functionalisation.

2.3 Adsorbent characterisation

Samples were dried for 2 h at 358K prior to coating with a thin layer (1.5 nm) of gold for Field Emission Scanning Electron Microscopy analysis (FE-SEM). A HITACHI SU-6600 (2010) microscope was used; the instrument is equipped with Energy Dispersive Spectroscopy (EDS), Oxford Inca 350 with 20 mm X-Max detector, Wavelength Dispersive Spectroscopy (WDS), and Oxford Inca Wave 700 Microanalysis System with Energy + Software. Surface areas, average pore sizes and pore size distributions were determined by nitrogen sorption measurements, performed at 77 K using a Micromeritics ASAP 2420. Samples were degassed at 393 K for 3-5 h, prior to analysis. Brunauer-Emmet-Teller (BET) (Brunauer et al., 1938) and Barret–Joyner–Halenda (BJH) methods (Barrett et al., 1951) were used to interpret the data obtained.

2.4 Adsorption studies

2.4.1 Batch adsorption

Virgin xerogels, fully functionalised xerogels and partially functionalised xerogels (obtained with 0.5 TMCS:Na_2SiO_3 ratio with respect to the fully functionalised samples) with ratios H_2O:Na_2SiO_3 between 138 and 154, were synthesised and used for batch adsorption tests with aqueous solutions of benzene and 3,4-DCA. Samples were ground to obtain particles with dimensions between 0.5 and 1.4 mm, prior to addition to glass bottles containing either aqueous benzene or aqueous 3,4-DCA; all solutions were previously equilibrated for 3 h with magnetic stirring. Bottles were subsequently placed in a Gerhardt® rotary stirrer for the determination of adsorption isotherms, and associated kinetics, as well as verification of the mechanical resistance of the materials. Adsorption batch tests on the amorphous silica Quartzene have been detailed in a previous work (Tasca et al., 2017).

2.4.2 Breakthrough curves

Samples were ground to obtain a particle size suitable for adsorption studies. Quartzene particles with average size of 140 µm and silica xerogel particles between 60 and 140 µm were used. A cylindrical microcolumn (length: 61.75 mm; internal diameter ID: 12.5 mm) was filled with adsorbent material and stoppered (pore size range 10 to 100 µm). UV-vis spectrophotometry was used for species detection, measuring the absorbance of the flowed solution at 254 and 255 nm for benzene and 3,4-DCA, respectively. The adsorption apparatus was positioned between a rotary valve and a UV-Vis detector, as presented in Figure 1.

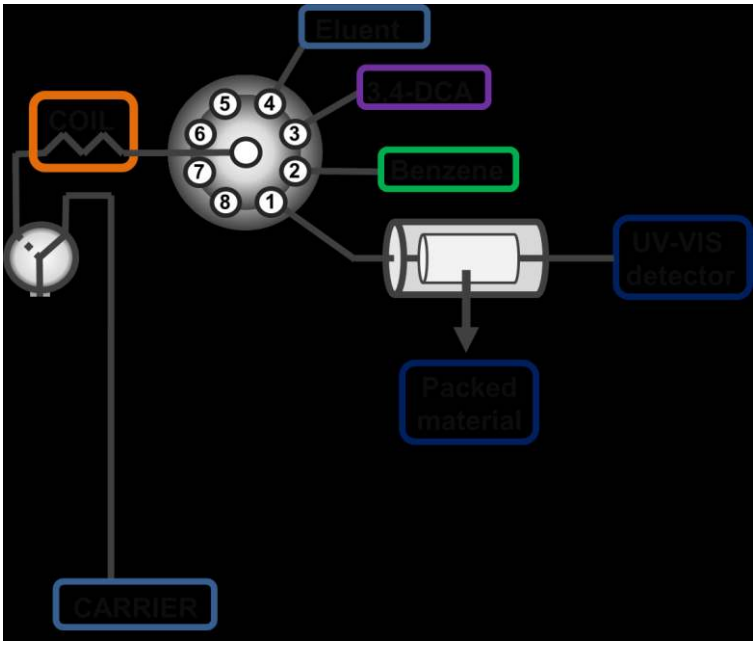

Figure 1: Sequential injection analysis manifolds connected to the adsorption column with a packed material and an on-line UV-Vis detector for adsorption tests on silica samples used in this study.

Compared to FIA, SIA employs a simpler, single-channel manifold for sample introduction, even with multi-component chemical systems; additionally, more accurate, robust syringe pumps are used in place of multi-channel peristaltic pumps. Through single-channel operation, the same manifold can be used to implement a wide range of assays and the rotary

valve enables automated calibration. Moreover, sample and reagent use are significantly reduced (Economou, 2005). In this study, using the aforementioned valve and a bidirectional syringe pump, water samples containing the target analyte were inserted into a loading coil (between the syringe and the central port of the valve), and subsequently injected towards the column. At the same time the detector begins recording the signal, in order to determine whether the analyte was fully retained in the column. Breakthrough curves are thus obtained, in order to establish both the volume and capacity of saturation. Automated solid-phase extraction was here also used to desorb the analytes from the exhausted adsorbents; whereby the procedure outlined above to obtain breakthrough curves was modified slightly, such that instead of loading a sample, methanol was loaded to promote desorption of the analyte once it was known to be fully retained within the column.

3 Results and discussion

3.1 3D printing of the column

Through the 3D modelling tool all the inside components of the column were individually created, as represented in Figure 2b. Working from the top of the column to the bottom they comprise:

- a 7 mm diameter cylinder of 7 mm length;
- a 1 mm diameter cylinder of 1 mm length;
- a truncated cone with 1 mm diameter top (to fit the previous tube) and 12.5 mm diameter base, with 5.75 mm height (to obtain the required 45° angle);
- a 12.5 mm diameter cylinder of 40 mm length (the inner column);
- a reverse truncated cone with 12.5 mm diameter base, height of 1 mm (to obtain the 20° angle) and 7 mm diameter base (not visible in Figure 2b);
- a 7 mm diameter cylinder of 7 mm length.

A Boolean union was used to combine the objects listed above into one solid piece; this command trims the shared areas of selected surfaces, creating a single polysurface from the unshared areas. The so-created inner part of the column (Figure 2b) was then fitted into a cylinder of 25 mm diameter and height equal to the sum of the heights of the previous parts (Figure 2a).

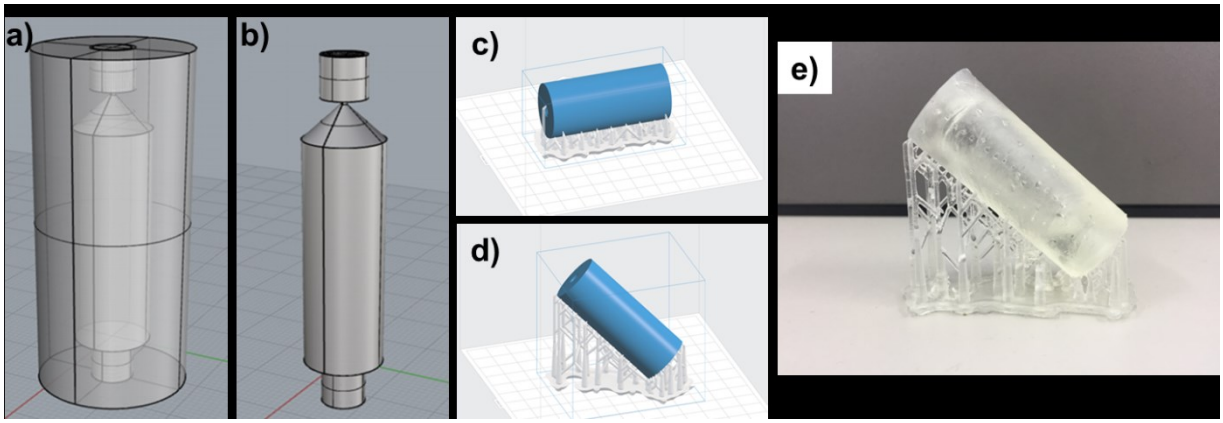

Figure 2: Inner column (b) and its fitting into the external cylinder (a). Models of the microcolumn and related supports (c,d), as shown by the software preform (FormLabs) and printed column on its supports, prior to smoothing (e).

Using a Boolean difference, which trims the shared areas of selected polysurfaces with another set of polysurfaces, the volume of the inside part of the model was extracted from the outside cylinder. Spirals were then designed in the inner part of the upper and lower cylinders of 7 mm diameter and 7 mm height, to permit fitting of the required connections. Once complete, the model was extracted as a STL file and sent to the 3D printer.

The STL file created was loaded in the software preForm, provided by FormLabs. The model was printed on clear methacrylate photopolymer resin by a Form1+ 3D printer from FormLabs (tech specs). After loading, two different orientations of the model, horizontal and inclined at 45°, were chosen, and related supports were added for correct printing. Figures 2c and 2d show the model in both orientations ready for printing.

The printing time for the model showed in Figure 2d was 4 h, requiring 31.41 ml of resin, while the model in Figure 2c required 1 h 38 min and 30.99 ml of resin due to the lower number of layers used in the print. The thickness of each layer was 0.1 mm. When each print was complete, the model was taken out of the printer, the supports were removed with a cutting tool, and the column was washed in isopropyl alcohol to eliminate any remaining liquid resin.

The penultimate processing step involved a CL-1000 ultraviolet crosslinker, used to cure the resin and remove the residual surface residue of methacrylate photopolymer and the associated 'tacky' sensation; finally a lathe was used to smooth the surface of the model.

3.2 Adsorbent characterisation

3.2.1 Quartzene

The structure of Quartzene and its properties are analogous to silica aerogels; all have porous skeletal silica structures, very low densities, and extremely low thermal conductivities. The major physical difference is that Quartzene is produced as a powder, not as a gel from a sol-gel process. FE-SEM analysis of ND samples is shown in Figure 3; Z1 samples show similar surface topography to ND, while the network of Quartzene CMS is quite different (Tasca et al., 2017).

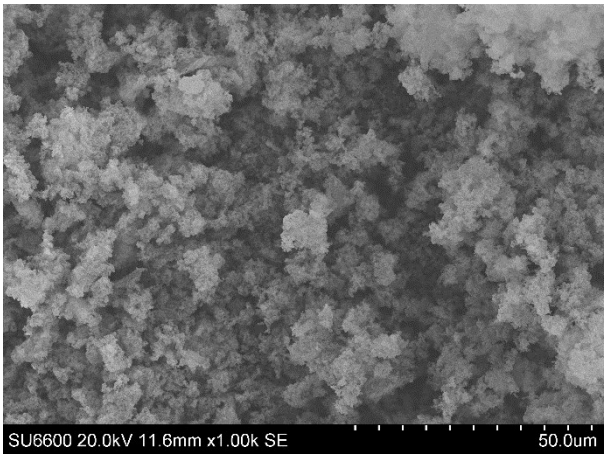

Figure 3: FE-SEM analysis of Quartzene ND. Magnification: x1k.

Detailed surface area and pore size analysis of Quartzene have been reported previously (Tasca et al., 2017); by comparison ND samples exhibit a higher surface area (546 m^2/g) and a narrower pore size distribution, with an average pore width of 3.3 nm. Samples CMS and Z1 have smaller surface areas, at 325 m^2/g and 158 m^2/g, respectively, and larger average pore widths of 20.3 nm and 14.6 nm, respectively.

3.2.2 Silica xerogels

FE-SEM analysis of virgin (non-functionalised) and functionalised silica xerogels are shown in Figure 4.

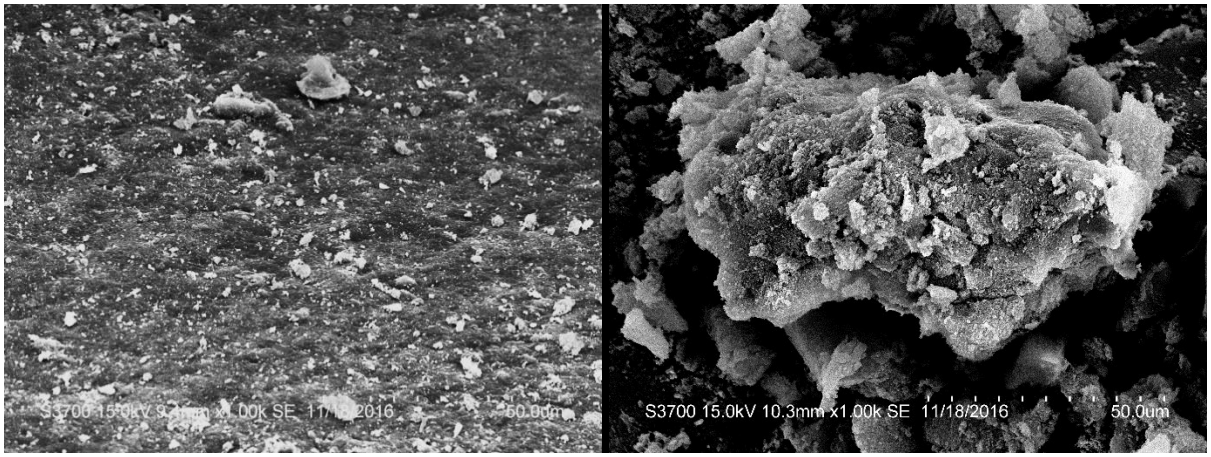

Figure 4: FE-SEM analysis of virgin xerogel (left) and functionalised xerogel (right) samples. Magnification: x1k.

Nitrogen sorption isotherms and the associated pore size distribution of the functionalised xerogel sample, obtained using H_2O:Na_2SiO_3 ratio equal to 154, are presented in Figure 5. The cooling time used after the last drying procedure was found to significantly affecting the porosity of the materials obtained; indeed, a rate of 10 K/min was initially used, while a gradient of 1 K/min was later found to increase the total pore volume of the samples, and was used in subsequent syntheses.

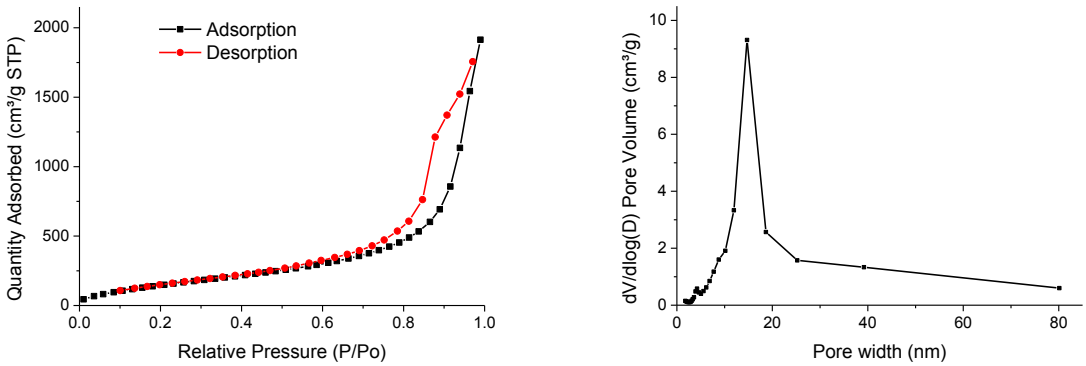

Figure 5: Adsorption isotherm (left) and pore size distribution (right) of functionalised xerogel sample.

Results for surface area and pore size analysis of functionalised xerogel samples obtained for H_2O:Na_2SiO_3 ratios between 80 and 154 are shown in Table 1; gels resulting from ratios ≥ 175, were too weak to undergo washing, as they dissolved in water. It is also notable that the main pore size distribution is considerably narrower for the lowest ratio examined.

Table 1: Surface area and porosity of xerogels obtained through citric acid catalysis, with different H_2O / Na_2SiO_3 ratios, fully functionalised.

Sample	Ratio n H_2O/n Na_2SiO_3	Surface Area m^2/g	Pore Volume cm^3/g	Pore Size nm	Pore size distribution nm
CF80	80	449.53	1.22	10.77	6.4 – 18
CF108	108	473.47	2.16	17.98	8.1 – 65
CF138	138	654.04	3.27	16.80	7-70
CF154	154	669.40	3.24	15.65	6.5 – 70

3.3 Adsorption studies

3.3.1 Batch adsorption

Quartzene

Results from batch adsorption studies using Quartzene ND, CMS, Z1 and Z1H have been discussed recently (Tasca et al., 2017). The majority of adsorption (84–90%) was observed to take place in the first 6 h of organics contact for CMS and ND samples, while Z1, tested in granular form, showed slower adsorption kinetics. The Freundlich adsorption model (Freundlich and Hatfield, 1926) fitted the data well and maximum adsorption capacity for ND was estimated as close to the adsorptive solubility limits at 264 mg/g for benzene. Under batch conditions, higher adsorption capacity was determined for the hydrophobic version of Z1 compared with its hydrophilic analogue (Z1H), however, the difference between the samples was seen to decrease with decreasing organic concentration. It was also noted that only hydrophobic samples showed no significant mechanical degradation post testing; hence, they could be suitable for multiple adsorption cycles. Recently an uptake of 50 mg/g was reached with the use of aerogels obtained from methyltrimethoxysilane (MTMS) as a

precursor and dried supercritically, immersed in aqueous solution of 50 mg/L of benzene (Perdigoto et al., 2012); an adsorption capacity of 2.5 mg/g of benzene was found for the Z1H sample at the same concentration of benzene, but the adsorption capacity increased sharply between 50 and 200 mg/L. Observations for Z1 are supported by batch results for CMS, which similarly showed a better performance for the hydrophobic version (CMSH) over all concentrations studied.

Silica xerogels

Kinetic tests on functionalised xerogels showed that they required long equilibrium times; only 50% of adsorption capacity was measured within 5 h, while full equilibrium required 2 d, for both benzene and 3,4-DCA. Non-functionalised and partially functionalised samples of xerogel, catalysed synthetically using citric acid, were unable to show sufficient mechanical resistance during the required tests, and were recovered as powder. It can, therefore, be concluded that non-fully functionalised sodium silicate xerogels synthesised under ambient pressure and at low temperature cannot be used for the uptake of organics in water in a filter configuration, while the functionalised analogous could be suitable to perform multiple adsorption cycles. Adsorption of benzene on functionalised xerogel samples exhibits Langmuir-Freundlich behaviour (Turiel et al., 2003) at concentrations >130 mg/L, while a Langmuir trend (Freundlich and Hatfield, 1926) can be used to describe the first adsorption points (Figure 6). A similar trend was recently observed for adsorption on mesoporous silica by Maretto *et al.* [1], who suggested a hybrid isotherm model, similar to that obtained by Lee *et al.* [2] for the adsorption of gaseous hydrocarbons on mesoporous silica MCM-48, in which the organic uptake at low concentrations is described by a Langmuir isotherm before shifting to Langmuir-Freundlich behaviour at concentrations >75 mg/L. As suggested for this gas adsorption system, the first step could be related to adsorption on the wall of the mesoporous channel until monolayer formation, in agreement

with the Langmuir model, with subsequent adsorption and formation of successive layers in agreement with the Langmuir-Freundlich model, until filling of the entire mesoporous channel occurs. Here, the results fit two separate models within specific concentration ranges better than the hybrid model proposed by Maretto *et al.*, which was based on adsorption data <150 mg/L and it is likely to underestimate the adsorption capacity of the silica xerogels beyond that threshold.

Adsorption tests with functionalised xerogels in an aqueous solution of 3,4-DCA confirmed Langmuir-Freundlich behaviour for concentrations >40 mg/L (Figure 6).

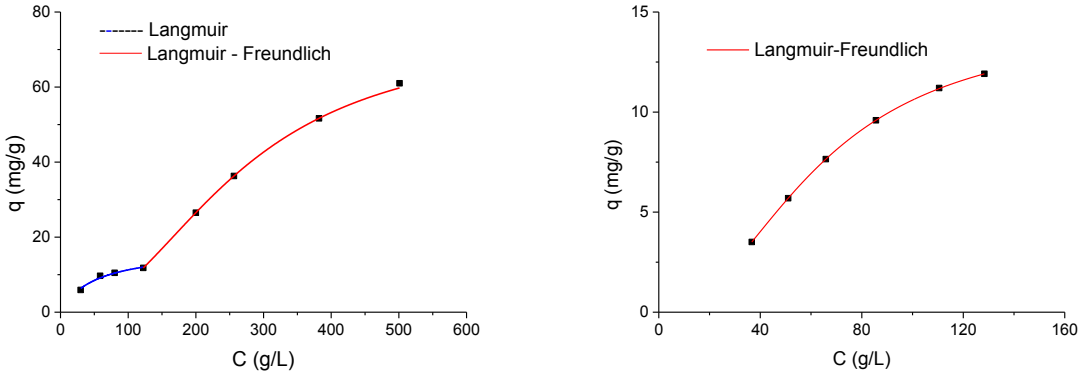

Figure 6: Adsorption isotherms for benzene (left) and 3,4-DCA (right) on xerogels with H_2O:Na_2SiO_3 ratio = 154.

The adsorption capacity of 3,4-DCA (12 mg/L) was found to be similar to benzene at concentrations of 130 mg/L but lower than benzene uptake at lower concentrations. Considering the solubility of 3,4-DCA and benzene at 293 K: 0.58 g/L and 1.77 g/L, respectively; it can be concluded that the adsorption trend of 3,4-DCA is similar to that obtained for benzene at concentrations between 130-600 mg/L, shifted to a lower range of concentrations (40-125 mg/L) as 3,4-DCA has a lower solubility limit. Indeed, 90% of the estimated maximum uptake is achieved at 130 mg/L for 3,4-DCA and at 600 mg/L for

benzene; thereby following the same adsorption trend from concentrations above ~8% of their solubility limits.

Table 2: Parameters of isotherms models.

	Langmuir			
	q_{max}(mg/g)	b (L/mg)		R^2
Benzene (<130 mg/L)	19.41	0.0155		0.9823
	Langmuir-Freundlich			
	Q_m(mg/g)	k_s (L/mg)	N	R^2
Benzene (>130 mg/L)	74.03	0.0038	2.1956	0.9997
3,4-DCA (≥ 40 mg/L)	14.43	0.0016	2.1462	0.9990

The intercept of the Langmuir-Freundlich plot of the data obtained for 3,4-DCA adsorption would be far from zero (Figure 6). Thus, further analyses could be useful to verify the presence of a two-step adsorption mechanism for the uptake of 3,4-DCA, as the one observed with benzene. Adsorption capacity of silica xerogels of 3,4-DCA was found greater than the uptake measured on the silicate minerals Halloysite (Szczepanik et al., 2014) Kaolinite and Montmorillonite (Angioi et al., 2005) in previous studies; difference is likely more related to the greater pore volume of xerogels and to its main role in the physical adsorption mechanism.

3.3.2 Breakthrough curves

30 mm x 7 mm (ID) and 61.75 mm x 12.5 mm (ID) columns were used and preliminary tests were conducted to evaluate the flow rate applicable without incurring overpressure (with consequent partial return of the flow in the sample container). Overpressure problems were experienced with the smaller column. Furthermore, channelling was less likely in the larger column, so the data reported here refer to the 3D printed 61.75 mm x 12.5 mm (ID) column. The materials were slightly swollen after flowing with methanol, with the increased volume notably maintained after washing with water. The sample solution organic concentration was determined, both during and at the end of the test, to confirm the absence of losses. For the

same reason, the sample was flowed through the system after disconnecting the column and again no significant losses were recorded. Hence, it can be assumed that the difference between the concentration of the organic in the solution before and after passing through the column it is due to adsorption on the packed material. Adsorption capacities were estimated by excluding the first 2 mL of sample flowed to wash the column from the water previously introduced and were limited to the uptake corresponding to the last point measured, so ~90% of the ratio C/C_0, where C_0 is the initial concentration of the organic in the solution flowed and C is the concentration of the organic in the solution leaving the column.

Quartzene

230 mg of NDH, provided with a particle size between 75 and 200 µm, were packed into the fabricated microcolumn, and a solution of 73.3 mg/g benzene in water was flowed through it at 1 mL/min. The flow rate selected equates to an $EBCT_{MC}$ (empty bed contact time of the microcolumn) of 1.47 min and to an $EBCT_{LC}$ (empty bed contact time of the large column) of 19.5 min, for a particle size of 0.5 mm to be employed in the bench scale reactor. The removal efficiency at $C/C_0 = 0.9$ was found to be 5.85 mg/g, i.e. insufficient to support scale up of the reactor.

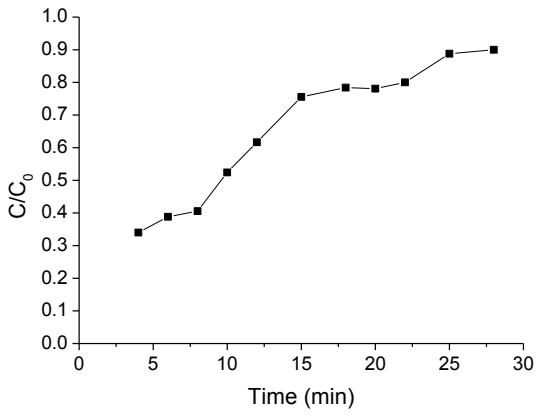

Figure 7: Breakthrough curve of benzene solution, 73.3 mg/L, flowed through microcolumn packed with 230 mg of NDH at 1 mL/min.

The analyte was successfully desorbed in less than 5 minutes by the use of automated solid-phase extraction, flowing methanol at 1 mL/min. Higher flow rates were not investigated, as even lower adsorption capacities would be expected, as contact time would be reduced. Higher removal efficiencies, coupled with no increase in $EBCT_{LC}$ would be required for the adsorbent tested to be used for treatment of produced water prior to a membrane configuration, especially in offshore facilities. However, as demonstrated from the high uptakes obtained in the batch test, the material could find applications in systems for which fast adsorption rate is not a priority.

Table 3: Parameters related to microcolumn tests with sample NDH (average particle size R_{SC} assumed equal to 0.014 mm and assuming 0.050 mm as particle size of the large column).

Adsorbent	Pollutant	Concentration mg/L	Rsc mm	$EBCT_{MC}$ min	$EBCT_{LC}$ min	Flowrate mL/min	Uptake mg/g
NDH	Benzene	73.3	0.14	1.47	19.5	1	5.85

Silica xerogels

110 mg of silica xerogel, catalysed with citric acid and with H_2O/Na_2SiO_3 ratio = 154, were packed into a microcolumn. The material was crushed and sieved to obtain particle sizes between 60 and 140 µm. A 105.12 mg/L benzene solution was flowed into the column at 0.6 mL/min; the related breakthrough curve is shown in Figure 8. The column was then packed with the same amount of adsorbent and solutions of 20 mg/L and 16 mg/L of 3,4-DCA were flowed at rates of 0.6 mL/min and 1.8 mL/min, respectively. Both the analytes

were then successfully desorbed within 5 minutes by the use of automated solid-phase extraction, flowing methanol at 1 mL/min.

The uptake of benzene at $C/C_0 = 0.9$ was 22.62 mg/g, and this significant removal efficiency is related to long $EBCT_{MC}$, thus, long $EBCT_{LC}$, during flow. Benzene adsorption was tested at selected concentrations, which were higher than those used for 3,4-DCA and in keeping with the range of interest for the offshore oil & gas sector probed in the present work. The sorbents studied here would not be competitive with hydrocyclones or flotators at concentrations of BTEX >100 mg/L, nor would they be competitive with nutshell or membrane for BTEX concentrations <20 mg/L.

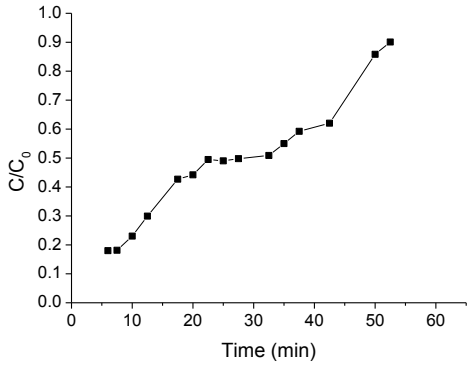

Figure 8: Breakthrough curve of benzene 105.12 mg/L at 0.6 mL/min, flowed through microcolumn packed with 110 mg of silica xerogels catalysed with citric acid and with H_2O/Na_2SiO_3 ratio = 154.

Greater flow rates, despite the corresponding reduction in adsorption capacity, could lead to a positive evaluation of the material for the use in a bench scale reactor; 1.8 mL/min was tested, but was judged unsuitable, as breakthrough curves started with values of $C/C_0 = 0.5$.

Silica xerogels synthetized here could then find an application for the adsorption of benzene, but only in systems for which fast adsorption rate is not a priority.

The uptake of 3,4-DCA was found to be >4.63 mg/g and >7.17 mg/g at flowrates of 1.8 mL/min and 0.6 mL/min, respectively; the breakthrough curves of the two runs are shown in Figure 9. The flowrate of 1.8 mL/min gives an $EBCT_{LC}$ of 20.5 min, considering 0.5 mm particles to be employed in the full scale reactor. The rate of adsorption, and the adsorption capacity of these silica xerogels, could be promising for a large scale application, as filling of filters, cartridges or permeable reactive barriers.

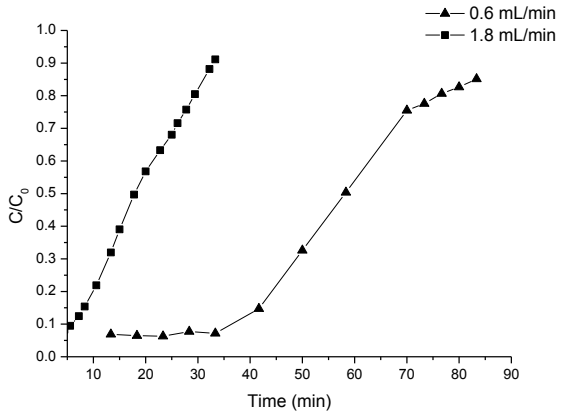

Figure 9: Breakthrough curves of 3,4-DCA adsorption on 110 mg of silica xerogels catalysed with citric acid and with H_2O/Na_2SiO_3 ratio = 154, 16 mg/L at 1.8 mL/min; 20 mg/L at 0.6 mL/min.

It is interesting to note that both the adsorption capacities obtained with column tests exceed those verified through batch test. This could be due to interparticle retention of the organic molecules and/or methanol conditioning prior to column packing.

Table 4: Parameters related to microcolumn tests using silica xerogels catalysed by citric acid (ratio H_2O/Na_2SiO_3 = 154), with average particle size R_{SC} of 0.01 mm and assuming 0.050 mm as particle size of large column.

Adsorbent	Pollutant	Concentration mg/L	Rsc mm	$EBCT_{MC}$ min	$EBCT_{LC}$ min	Flowrate mL/min	Uptake mg/g
Silica xerogel	benzene	105.1	0.1	2.44	61	0.6	5.85
	3,4-DCA	20	0.1	2.44	61	0.6	7.17
	3,4-DCA	16	0.1	0.83	20.7	1.8	4.63

4 Conclusions

The MCRB test coupled with Sequential Injection Analysis and automated solid-phase extraction have employed to analyse the adsorption performance of the materials studied here, to assess their treatment effectiveness, to estimate the capacity utilisation rate and regeneration options.

The developed materials could find application in filtration vessels in oil and gas plants for removal of dissolved oils or as filling of cartridges for the same purpose, as stand-alone technology, or prior to a membrane configuration, extending the membrane lifetime. Functionalised silica could also be used for the removal of 3,4-DCA and other EDCs in drinking water treatment facilities, as well as sorbents for the in-situ remediation of pesticides-polluted groundwater as part of permeable reactive barriers.

Acknowledgements

The authors would like to thank Svenska Aerogel AB for providing the adsorbent material Quartzene.

References

Adebajo, M. O., Frost, R. L., Kloprogge, T. J., Carmody, O. and Kokot, S., Porous Materials for Oil Spill Cleanup: A Review of Synthesis and Absorbing Properties, Journal of Porous Materials, vol. 10**,** pp. 159-170, 2003.

Angioi, S., Polati, S., Roz, M., Rinaudo, C., Gianotti, V. and Gennaro, M. C., Sorption studies of chloroanilines on kaolinite and montmorillonite, Environmental Pollution, vol. 134**,** pp. 35-43, 2005.

Astm 2008. Standard Practice for the Prediction of Contaminant Adsorption On GAC In Aqueous Systems Using Rapid Small-Scale Column Tests.

Bangi, U. K. H., Rao, A. P., Hirashima, H. and Rao, A. V., Physico-chemical properties of ambiently dried sodium silicate

based aerogels catalyzed with various acids, Journal of sol-gel science and technology, vol. 50**,** pp. 87-97, 2009.

Barrett, E. P., Joyner, L. G. and Halenda, P. P., The determination of pore volume and area distributions in porous substances .1. Computations from nitrogen isotherms, J. Am. Chem. Soc., vol. 73**,** pp. 373-380, 1951.

Bevan, R., Harrison, P., Youngs, L., Whelan, M., Goslan, E., Macadam, J., Holmes, P. and Persich, T. 2012. A review of latest endocrine disrupting chemicals research implications for drinking water.

Brunauer, S., Emmett, P. H. and Teller, E., Adsorption of Gases in Multimolecular Layers, J. Am. Chem. Soc., vol. 60**,** pp. 309-319, 1938.

Chang, Q. G., Zhang, W., Jianga, W. X., Li, B. J., Yinga, W. C. and Lin, W., Efficient micro carbon column rapid breakthrough technique for water and wastewater treatability studies, Environ. Prog., vol. 26**,** pp. 280-288, 2007.

Economou, A., Sequential-injection analysis (SIA): A useful tool for on-line sample-handling and pre-treatment, TrAC Trends in Analytical Chemistry, vol. 24**,** pp. 416-425, 2005.

Falkova, M., Vakh, C., Shishov, A., Zubakina, E., Moskvin, A., Moskvin, L. and Bulatov, A., Automated IR determination of petroleum products in water based on sequential injection analysis, Talanta, vol. 148**,** pp. 661-665, 2016.

Freundlich, H. and Hatfield, H. 1926. Colloid and Capillary Chemistry, London, Methuen.

Hampson, S. M., Rowe, W., Christie, S. D. R. and Platt, M., 3D printed microfluidic device with integrated optical sensing for particle analysis, Sens. Actuator B-Chem., vol. 256**,** pp. 1030-1037, 2018.

Hwa, L. C., Rajoo, S., Noor, A. M., Ahmad, N. and Uday, M. B., Recent advances in 3D printing of porous ceramics: A review, Current Opinion in Solid State & Materials Science, vol. 21**,** pp. 323-347, 2017.

Kortenkamp, A., Faust, M., Scholze, M. and Backhaus, T., Low-Level Exposure to Multiple Chemicals: Reason for Human Health Concerns?, Environ. Health Perspect., vol. 115**,** pp. 106-114, 2007.

Mitsouras, D., Liacouras, P., Imanzadeh, A., Giannopoulos, A. A., Cai, T. R., Kumamaru, K. K., George, E., Wake, N., Caterson, E. J., Pomahac, B., Ho, V. B., Grant, G. T. and Rybicki, F. J., Medical 3D Printing for the Radiologist, Radiographics, vol. 35**,** pp. 1966-1989, 2015.

Olalekan, A. P., Dada, A. O. and Adesina, O. A., Review: Silica Aerogel as a Viable Absorbent for Oil Spill Remediation, Journal of Encapsulation and Adsorption Sciences, vol. 4**,** pp. 122-131, 2014.

Perdigoto, M. L. N., Martins, R. C., Rocha, N., Quina, M. J., Gando-Ferreira, L., Patrício, R. and Durães, L., Application of hydrophobic silica based aerogels and xerogels for removal of toxic organic compounds from aqueous solutions, J. Colloid Interface Sci., vol. 380**,** pp. 134-140, 2012.

Reynolds, J. G., Coronado, P. R. and Hrubesh, L. W., Hydrophobic aerogels for oil-spill clean up – synthesis and characterization, Journal of Non-Crystalline Solids, vol. 292**,** pp. 127-137, 2001a.

Reynolds, J. G., Coronado, P. R. and Hrubesh, L. W., Hydrophobic aerogels for oil-spill cleanup - Intrinsic absorbing properties, Energy Sources, vol. 23**,** pp. 831-843, 2001b.

Rodríguez, R., Avivar, J., Leal, L. O., Cerdà, V. and Ferrer, L., Strategies for automating solid-phase extraction and liquid-liquid extraction in radiochemical analysis, TrAC Trends in Analytical Chemistry, vol. 76**,** pp. 145-152, 2016.

Shu, H. C. and Chung, S. W., Analysis of Organophosphorous Pesticides Based on Housefly Acetylcholinesterase Using Sequential Injection Analysis, J. Chin. Chem. Soc., vol. 64**,** pp. 1460-1466, 2017.

Simpson, E. J., Abukhadra, R. K., Koros, W. J. and Schechter, R. S., Sorption Equilibrium Isotherms for Volatile Organics in Aqueous-Solution - Comparison of Headspace Gas-Chromatography and Online Uv Stirred Cell Results, Ind. Eng. Chem. Res., vol. 32**,** pp. 2269-2276, 1993.

Szczepanik, B., Slomkiewicz, P., Garnuszek, M. and Czech, K., Adsorption of chloroanilines from aqueous solutions on the modified halloysite, Applied Clay Science, vol. 101**,** pp. 260-264, 2014.

Tasca, A. L., Ghajeri, F. and Fletcher, A. J., Novel hydrophilic and hydrophobic amorphous silica: Characterization and adsorption of aqueous phase organic compounds, Adsorption Science & Technology, vol.**,** pp., 2017.

Turiel, E., Perez-Conde, C. and Martin-Esteban, A., Assessment of the cross-reactivity and binding sites characterisation of a propazine-imprinted polymer using the Langmuir-Freundlich isotherm, Analyst, vol. 128**,** pp. 137-141, 2003.

Twumasi Afriyie, E., Karami, P., Norberg, P. and Gudmundsson, K., Textural and thermal conductivity properties of a low density mesoporous silica material, Energy and Buildings, vol. 75**,** pp. 210-215, 2014.

Twumasi Afriyie, E., Norberg, P., Sjöström, C. and Forslund, M., Preparation and Characterization of Double Metal-Silica Sorbent for Gas Filtration, Adsorption, vol. 19**,** pp. 49-61, 2013.

Wang, D., Mclaughlin, E., Pfeffer, R. and Lin, J. Y. S., Adsorption of Organic Compounds in Vapor, Liquid, and Aqueous Solution Phases on Hydrophobic Aerogels, Ind. Eng. Chem. Res., vol. 50**,** pp. 12177-12185, 2011.

Wang, D., Mclaughlin, E., Pfeffer, R. and Lin, J. Y. S., Adsorption of oils from pure liquid and oil-water emulsion on hydrophobic silica aerogels, Separation and Purification Technology, vol. 99**,** pp. 28-35, 2012.

Ying, W. C., Zhang, W., Chang, Q. G., Jiang, W. X. and Li, G. H., Improved methods for carbon adsorption studies for water and wastewater treatment, Environ. Prog., vol. 25**,** pp. 110-120, 2006.